Relativistic versus nonrelativistic optical potentials in $A(e,e'p)B$ reactions

J. M. Udías,[1] P. Sarriguren,[2] E. Moya de Guerra,[2] E. Garrido,[2] and J. A. Caballero[2]
[1]*National Laboratory for Nuclear and High-Energy Physics, Section K (NIKHEF-K), P.O. Box 41882, 1009 DB Amsterdam, The Netherlands*
[2]*Instituto de Estructura de la Materia, Consejo Superior de Investigaciones Científicas, Serrano 119, E-28006 Madrid, Spain*
(Received 16 January 1995)

We investigate the role of relativistic and nonrelativistic optical potentials used in the analysis of $(e,e'p)$ data. We find that the relativistic calculations produce smaller $(e,e'p)$ cross sections even in the case in which both relativistic and nonrelativistic optical potentials fit equally well the elastic proton-nucleus scattering data. Compared to the nonrelativistic impulse approximation, this effect is due to a depletion in the nuclear interior of the relativistic nucleon current, which should be taken into account in the nonrelativistic treatment by a proper redefinition of the effective current operator.

PACS number(s): 25.30.Fj, 24.10.Jv, 21.10.Jx

I. INTRODUCTION

The quasielastic $(e,e'p)$ reaction has been extensively studied over the last years as a powerful tool to obtain information on the momentum distribution of the nuclear bound states and to extract experimental information on absolute spectroscopic factors.

Although high precision measurements of cross sections for this reaction are already available [1–3], the extraction of spectroscopic factors from experiment is still not free of ambiguities. The origin of the uncertainty has to be found in the complexity of the reaction and the different approaches proposed to handle it, which produce different cross sections even within the impulse approximation (IA) scheme considered here. It is clear that a reliable determination of spectroscopic factors requires an accurate description of the mechanism of the reaction.

One major puzzle at present is the discrepancy between spectroscopic factors obtained from relativistic and nonrelativistic analyses of data.

Traditionally, differential cross sections for quasielastic electron-nucleus scattering have been calculated using nonrelativistic approaches to the nuclear currents. The analyses of $(e,e'p)$ data are generally made (see Refs. [1–3] and references therein) within this nonrelativistic framework using the DWEEPY program [4,5], which provides a rather complete description of the process. A fully relativistic formalism for the quasielastic $(e,e'p)$ reaction has appeared over the last years [6–8], and applications to the extraction of spectroscopic factors comparing with the experimental data have become available recently [9–11].

The typical values of the spectroscopic factors obtained within these relativistic analyses (about 70% for the $3s_{1/2}$ state in ^{208}Pb) are much larger than those obtained in the nonrelativistic analyses (about 50% for the same shell as above [2]). These higher values are consistent with theoretical predictions [12] as well as with the spectroscopic factors obtained from other methods [13]. Yet, the difference with respect to the nonrelativistic results is distressing and remains to be explained.

In Ref. [11] we studied the differences between the relativistic and the nonrelativistic treatments of the $(e,e'p)$ reaction and, in particular, we investigated the causes leading to the discrepancies found in the spectroscopic factors obtained in the two formalisms. Two different aspects of the analysis were identified in said reference as the main sources of discrepancy. First, the treatment of the Coulomb distortion of the electron, which at present is only exact within a relativistic formalism. We demonstrated that a complete treatment of this distortion is necessary in order to obtain reliable spectroscopic factors in heavy nuclei. Second, the different quenching of the $(e,e'p)$ cross section produced by the relativistic and the nonrelativistic optical potentials, which are introduced to take into account final state interactions. We showed that this quenching can differ typically by 15%, even though both relativistic and nonrelativistic optical potentials fit the elastic proton-nucleus scattering data for the particular proton energies and mass target nuclei under study. In this paper we elaborate more on this last point.

The optical potentials used in $(e,e'p)$ are generally determined from elastic nucleon-nucleus scattering data. It is well known that these data are only sensitive to the asymptotic behavior of the wave functions. Wave functions that are different in the nuclear interior but are identical in the asymptotic region give rise to equal elastic observables. However, this is not necessarily the case for inelastic (p,p') scattering or for $(e,e'p)$ reactions.

In Ref. [14] it was shown that the results for inelastic (p,p') scattering may differ when using different optical potentials that give nearly equivalent fits to the elastic observables. In particular, in that reference, results obtained with a Dirac-equation-based (DEB) optical potential were presented. As discussed in the next section, the DEB potential is obtained from the relativistic optical potential when the Dirac equation is transformed into a Schrödinger-like equation for the upper component. Though derived in this particular way, the DEB potential can be used in the nonrelativistic formalism as

another phenomenological optical potential. The advantage of treating the DEB potential on the same footing as other nonrelativistic optical potentials is that with this potential the Schrödinger equation produces the same elastic scattering as the Dirac equation.

Concerning the $(e,e'p)$ process, several questions have emerged in the last years, namely (i) to what extent different optical potentials fitted to elastic proton-nucleus scattering data may differ in their predictions on $(e,e'p)$ cross sections, (ii) what are the features of these optical potentials to which the $(e,e'p)$ reaction is sensitive while elastic proton-nucleus scattering is not, (iii) is the nuclear interior probed by the $(e,e'p)$ reaction responsible for the discrepancies found between the relativistic and the nonrelativistic approaches? In this context, some properties of final state interactions and optical potentials have been already studied within a nonrelativistic framework. In Ref. [15], the role of nonlocality in the treatment of final state interactions and its effect on the extracted occupation numbers from $(e,e'p)$ was investigated, and the estimated effect was about a 15% increase in the occupation probabilities. In Ref. [16] a phenomenological analysis was carried out to show that the $(e,e'p)$ cross sections are sensitive to the behavior of the optical potential in the nuclear interior. In this last reference it was also argued that an increased absorption in the nuclear interior, with respect to the absorption produced by the traditional parametrization of the optical potentials, is more consistent both with $(e,e'p)$ data and with microscopic calculations of the optical potentials. These arguments were already taken into account in constructing the nonrelativistic optical potentials given in Refs. [2,3] and used in this work under the name standard nonrelativistic optical potentials.

In this paper we compare the $(e,e'p)$ differential cross section obtained with the nonrelativistic treatment provided by the DWEEPY program using different nonrelativistic optical potentials, as well as with the results obtained with the fully relativistic treatment [11]. We show that the results for $(e,e'p)$ with relativistic and nonrelativistic optical potentials differ even in the case in which both types of potentials give exactly the same results for elastic proton-nucleus scattering. We also explore the reasons for the discrepancies.

The paper is organized as follows. In Sec. II we discuss the choices taken for the optical potentials within the relativistic and the nonrelativistic formalisms, and what are their distinguishing features, focusing on ^{208}Pb. In Sec. III we summarize briefly the relativistic and nonrelativistic formalisms used in this work, and discuss the results for $(e,e'p)$ cross sections for ^{208}Pb obtained with various potentials. Some results for ^{40}Ca are also given. In Sec. IV we present the main conclusions.

II. RELATIVISTIC AND NONRELATIVISTIC OPTICAL POTENTIALS

The usual procedure to take into account final state interactions in the $(e,e'p)$ reaction is to introduce as input a phenomenological optical potential with parameters fitted to reproduce elastic proton-nucleus scattering data. Two different approaches are widely used in the construction of the optical potentials, which correspond to relativistic or nonrelativistic descriptions of the proton-nucleus scattering. Though microscopically derived optical potentials are available in the literature (for a recent review see Ref. [17]), in this work we use empirical parametrizations. As in our previous work [11], we use phenomenological optical potentials based on complex central and spin-orbit potentials, in the nonrelativistic case, and on standard Lorentz scalar and timelike vector complex terms (S-V) in the Dirac phenomenology.

To be specific, in the relativistic case we use the parametrization denoted as fit 2 in Ref. [18] of the scalar (U_S), vector (U_V), and Coulomb (U_C) potentials to solve the time independent Dirac equation in configuration space:

$$[i\boldsymbol{\alpha}\cdot\boldsymbol{\nabla}-\beta(M+U_S)+E-U_V-U_C]\Psi=0\ , \quad (2.1)$$

where $\Psi\equiv(\Psi_{\rm up},\Psi_{\rm down})$ is a Dirac four spinor. The potentials of Ref. [18] are obtained from global fits whose parameters are functions of both projectile energy and target mass number. The parameters have been fitted to elastic proton-nucleus observables (cross sections, analyzing powers, and spin rotation functions) and the range of applicability covers spherical nuclei with mass numbers $40< A <208$, and energies 65 MeV $< E <$ 1040 MeV. A new parametrization has been reported recently [19], extending the range of applicability to 20 MeV and including ^{12}C and ^{16}O in the fit. For the mass number and proton energy of our concern here, the agreement with experiment is comparable to that of Ref. [18].

In the nonrelativistic treatment we use for the outgoing proton the solutions of the Schrödinger equation with two types of potentials: (i) the DEB potential, obtained from the relativistic one as discussed below, and (ii) the phenomenological parametrization of Ref. [2], involving Coulomb, complex central, imaginary surface, and complex spin-orbit terms:

$$\begin{aligned}U(r)=&-V_C(r,R_C)-Vf(x_V)\\&-iWf(x_W)+4ia_SW_Sf(x_S)\\&+(2/r)[V_{\rm SO}f'(x_{\rm SO})+iW_{\rm SO}f'(x_{\rm WSO})]\boldsymbol{\sigma}\cdot\boldsymbol{l}, \quad (2.2)\end{aligned}$$

where $x_i=(r-R_i)/a_i$ $(i=V,W,S,{\rm SO},{\rm WSO},C)$, $R_i=r_i(A-1)^{1/3}$, $f'(x)=df(x)/dx$, $f(x)$ is the standard Woods-Saxon function, $V_C(r,R_C)$ is the Coulomb potential of a homogeneously charged sphere with radius $R_C=\sqrt{5/3}\langle r^2\rangle^{1/2}$. The parameters are given in Table I.

The DEB potential is obtained by rewriting the Dirac equation [Eq. (2.1)] as a second order differential equation for the upper component (see Appendix A) to obtain the equivalent Schrödinger equation:

$$\left[-\frac{\boldsymbol{\nabla}^2}{2M}-U_{\rm DEB}\right]\phi(\mathbf{r})=E_{\rm nr}\phi(\mathbf{r})\ , \quad (2.3)$$

with $E_{\rm nr}=(E^2-M^2)/2M$ and $\phi(\mathbf{r})$ a bispinor. This is the standard procedure [14] used to analyze the relation-

TABLE I. Parameters of the standard nonrelativistic optical potentials for ^{208}Pb and ^{40}Ca from Refs. [2] and [3], respectively. Depths are in MeV and distances in fm.

	V	W	W_S	V_{SO}	W_{SO}
^{208}Pb	27.93	9.000	3.16	4.000	-0.835
^{40}Ca	26.97	7.177	0.	4.379	-1.066
	r_V	r_W	r_S	r_{SO}	r_{WSO}
^{208}Pb	1.223	1.137	1.272	1.116	1.088
^{40}Ca	1.225	1.410		1.034	0.999
	a_V	a_W	a_S	a_{SO}	a_{WSO}
^{208}Pb	0.719	0.742	0.622	0.676	0.719
^{40}Ca	0.706	0.570		0.648	0.620

ship between the large S-V potentials in the Dirac phenomenology, and the usual spin independent and spin-orbit potentials in the Schrödinger equation. As it is known [14], the DEB potential contains an effective central potential that results from a partial cancellation between the S-V relativistic potentials plus important quadratic terms, and a spin-orbit potential that originates from additive contributions from the S-V potentials:

$$U_{\rm DEB} = V_C + V_{\rm so}\boldsymbol{\sigma}\cdot\boldsymbol{l}\,, \tag{2.4}$$

where

$$V_C = \frac{1}{2M}[(U_V+U_C)2 - 2E(U_V+U_C) - U_S^2 \\ -2MU_S + V_D]\,, \tag{2.5}$$

with

$$V_D = \frac{1}{rA}\frac{\partial A}{\partial r} + \frac{1}{2A}\frac{\partial^2 A}{\partial r^2} - \frac{3}{4A^2}\left(\frac{\partial A}{\partial r}\right)^2\,, \tag{2.6}$$

$$A(r) = \frac{E - U_V - U_C + M + U_S}{E+M}\,, \tag{2.7}$$

and

$$V_{\rm so} = \frac{1}{2M}\frac{1}{rA}\frac{\partial A}{\partial r}\,. \tag{2.8}$$

A well-known feature of this procedure [17] is that the DEB potentials, and in particular the real central part, show a more dramatic energy dependence than the standard potentials with Woods-Saxon shapes. This is especially important for proton energies larger than ~200 MeV where the real central DEB potential weakens its attraction in the interior of the nucleus but not at the surface [17]. The departure from standard Woods-Saxon shapes is characteristic of the Dirac approach, and is due to the presence of nonlinear terms in the central potential. Even when the S-V potentials have standard Woods-Saxon shapes, the nonrelativistic potentials obtained from them will in general have nonstandard geometries. Although these changes start to be sizable above proton energies of 200 MeV, they are also present to a lower extent at the energies of interest in this work [100 MeV for the ejected proton in the $(e,e'p)$ reaction].

Figure 1 contains the real and imaginary parts of the DEB potential, for the particular case of ^{208}Pb and for a proton energy of 100 MeV, compared with the standard nonrelativistic optical potential given by Eq. (2.2) and Table I. The DEB potential has been obtained using Eqs. (2.5)–(2.8) and the phenomenological S-V relativistic potential of fit 2 in Ref. [18], calculating the Coulomb potential U_C from the empirical charge distribution of the target nucleus, as it is done in said reference. As can be seen from Fig. 1 the real central potentials, which include the Coulomb contributions, are similar in shape at this energy, DEB being deeper in the interior and more repulsive at the surface. The depth of the imaginary central potential is also larger for DEB showing a departure from a Woods-Saxon shape near the surface. We have checked that these features prevail independently on whether we use fit 1 or fit 2 of Ref. [18], or even the energy-dependent A-independent fit of Ref. [19], for the nucleus and energy considered here. Actually these three fits produce very similar fully relativistic $(e,e'p)$ cross sections [20]. It should be mentioned, however, that the imaginary part of the DEB central potential varies for these three fits, and depends more than the real part on the particular choice of the S-V relativistic potential. For the three fits mentioned above, the real parts of V_C are practically identical, while the imaginary parts have

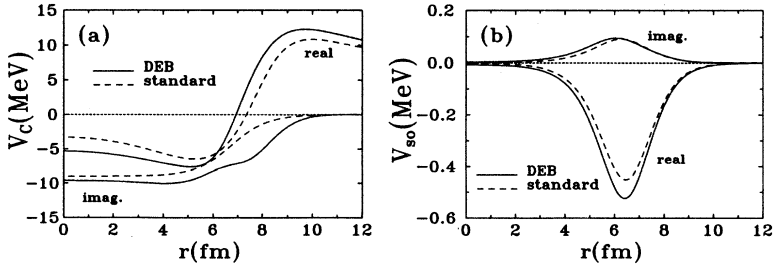

FIG. 1. Nonrelativistic central (V_C) and spin-orbit ($V_{\rm so}$) optical potentials for ^{208}Pb and 100 MeV proton energy. Solid lines correspond to the potentials [Eqs. (2.5)–(2.8)] obtained after the reduction of the Dirac equation with the S-V relativistic optical potentials of Ref. [18]. Dashed lines correspond to the Schrödinger optical model with the parameters of Ref. [2].

somewhat different depths. We consider here fit 2 because the imaginary part of V_C produced by fit 2 is the shallowest and closest to the standard potential.

The spin-orbit potentials show a similar shape in both the DEB and standard potentials, with a somewhat larger strength for DEB.

Clearly the comparison in Fig. 1 is useful to understand the relationship between results obtained in the nonrelativistic treatment of $(e,e'p)$ with DEB and standard optical potentials, as discussed in next section. In addition, using the DEB potential helps to understand the relationship between results of relativistic and nonrelativistic treatments.

It can be shown (see Appendix A) that the solution of the equivalent Schrödinger equation [Eq. (2.3)] is related to the upper component of the solution of the Dirac equation [Eq. (2.1)] by

$$\Psi_{\rm up}(\mathbf{r}) = K(r)\phi(\mathbf{r}) \tag{2.9}$$

with

$$K(r) = A^{1/2}(r)\ . \tag{2.10}$$

In Fig. 2 we show the real and imaginary parts of $A(r)$ as obtained from Eq. (2.7). The imaginary part is very small and has been neglected in the subsequent calculations. The real part is clearly different from unity in the interior of the nucleus. We get a steady value of about 0.63 [$K(r) \sim 0.79$] in the interior going to unity asymptotically.

Thus the distorted wave $\phi(\mathbf{r})$ generated by the DEB potential is equal to the upper component of the Dirac equation only asymptotically [$\lim_{r\to\infty} K(r) = 1$]. This means that Eq. (2.1) and Eq. (2.3) will produce the same elastic proton-nucleus observables, which are only sensitive to this asymptotic behavior, but for processes where the nuclear interior plays a role, both equations can lead to different results. On the other hand, solving the Schrödinger equation (2.3) for $\phi(\mathbf{r})$ and using the Darwin factor $K(r)$ is equivalent to solving the Dirac equation (2.1) for $\Psi_{\rm up}(\mathbf{r})$. Hence, comparing results for $(e,e'p)$ with relativistic and nonrelativistic treatments based on the same relativistic potential allows us to disentangle effects due to different features of the optical potentials from effects due to the fully relativistic treatment.

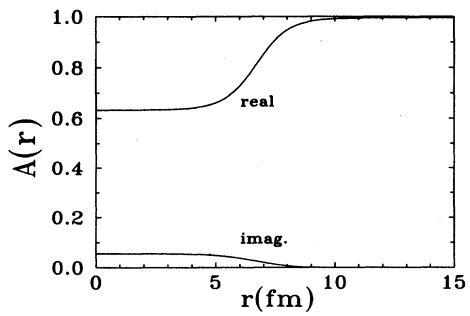

FIG. 2. Real and imaginary parts of $A(r)$ in Eq. (2.7) using the S-V relativistic optical potentials of Ref. [18] for ^{208}Pb and 100 MeV proton energy.

III. RESULTS FOR $(e,e'p)$ CROSS SECTIONS

In this section we first summarize briefly the formalism used to describe the $(e,e'p)$ reaction both relativistically and nonrelativistically. More details can be found in Refs. [10,11,20]. We base our calculations on the impulse approximation (virtual photon absorbed by the detected nucleon), which is known [21] to be a reliable approximation at quasielastic kinematics.

In Refs. [9–11,20] it has been shown the importance of treating correctly the electron Coulomb distortion, especially in heavy targets, in order to obtain reliable spectroscopic factors from experiment. For the purpose of this work it is, however, advantageous to switch off the electron Coulomb distortion, treating the electron current in the plane wave Born approximation (PWBA). The reasons for this are that the role of the various optical potentials stands out more clearly and that at present the electron Coulomb distortion cannot be treated exactly within the nonrelativistic framework. Hence, in this work all the calculations are made in PWBA (no electron Coulomb distortion) and the differences in the results presented come only from the various approximations to the nuclear current. In impulse approximation, differences between relativistic and nonrelativistic analyses can occur due to the bound nucleon wave function, to the current operator, or to the final nucleon wave function in the γNN vertex. Therefore, we first discuss the choice of these ingredients within the two formalisms.

All the results in this section correspond to $(e,e'p)$ reduced cross sections in parallel kinematics (momentum transfer parallel to missing momentum, $\mathbf{q} \parallel \mathbf{p}$) with a fixed value of the kinetic energy of the outgoing proton (T_F =100 MeV). Since these results do not include electron Coulomb distortion, we do not compare them with experiment (for such a comparison see Ref. [11]).

A. Relativistic formalism

Results for the $(e,e'p)$ reaction obtained through a fully relativistic formalism have appeared in recent years, either computing the nuclear matrix elements in configuration space [9–11] or in momentum space [6–8]. While the latter formalism may be somewhat more elegant and better suited to deal with p-dependent terms in the current operator, the first one is more adequate when the Coulomb distortion of the electron wave functions has to be taken into account.

For the relativistic formalism in configuration space that we use here, the basic equations that determine the reduced cross section are given explicitly in Refs. [10,11], in terms of the electron and nuclear currents. The calculations have been performed with the relativistic code developed by one of us [20]. We give here the basic equations in PWBA.

We work in the laboratory frame in which the target nucleus is at rest and use the notation and conventions of Ref. [22]. We denote by $k_i^\mu = (\epsilon_i, \mathbf{k}_i)$ the four-momentum of the incoming electron and by $k_f^\mu = (\epsilon_f, \mathbf{k}_f)$ the four-momentum of the outgoing one. The four-momentum

of the exchanged photon is $q^\mu = k_i^\mu - k_f^\mu = (\omega, \mathbf{q})$. $P_A^\mu = (M_A, \mathbf{0})$ and $P_{A-1}^\mu = (E_{A-1}, \mathbf{P}_{A-1})$ denote the four-momenta of the target and residual nucleus, while $P_F^\mu = (E_F, \mathbf{P}_F)$ is the four-momentum of the ejected proton.

Using plane waves for the electrons and considering knockout from a given $\{nlj\}$ shell, we write the amplitude for the $(e, e'p)$ process in distorted-wave impulse approximation (DWIA) as [11,20,21]

$$W_{if} = \frac{m_e}{\sqrt{\epsilon_i \epsilon_f}} \bar{u}(\mathbf{k}_f, \sigma_f) \gamma_\mu u(\mathbf{k}_i, \sigma_i) \frac{(-1)}{q_\mu^2} \sqrt{N_{\{nlj\}}} J_N^\mu(\omega, \mathbf{q}) \ , \tag{3.1}$$

where $u(\mathbf{k}, \sigma)$ represent four-component relativistic free electron spinors [22], $N_{\{nlj\}}$ is the occupation number of the $\{nlj\}$ shell, and $J_N^\mu(\omega, \mathbf{q})$ is the nucleon current

$$J_N^\mu(\omega, \mathbf{q}) = \int d\mathbf{y} \, e^{i\mathbf{q}\cdot\mathbf{y}} \bar{\Psi}_F(\mathbf{y}) \hat{J}_N^\mu \Psi_B(\mathbf{y}) \ , \tag{3.2}$$

where Ψ_B and Ψ_F are the wave functions for the initial bound nucleon and for the outgoing final nucleon, respectively, and $\hat{J}_N^\mu$ is the nucleon current operator to be specified later. These are the three ingredients that change when one considers a relativistic treatment or a nonrelativistic one.

Within the relativistic framework the bound state wave function for the proton, Ψ_B, is a four-spinor with well defined angular momentum quantum numbers $\kappa_B \mu_B$ corresponding to the shell under consideration. We use four-spinors of the form

$$\Psi_\kappa^\mu(\mathbf{r}) = \begin{pmatrix} g_\kappa(r) \phi_\kappa^\mu(\hat{r}) \\ i f_\kappa(r) \phi_{-\kappa}^\mu(\hat{r}) \end{pmatrix} \tag{3.3}$$

that are eigenstates of total angular momentum with eigenvalue $j = |\kappa| - 1/2$,

$$\phi_\kappa^\mu(\hat{r}) = \sum_{m,\sigma} \langle l \ m \ \tfrac{1}{2} \ \sigma | \ j \ \mu \rangle Y_{lm}(\hat{r}) \chi_\sigma^{\frac{1}{2}} \tag{3.4}$$

with $l = \kappa$ for $\kappa > 0$, $l = -\kappa - 1$ for $\kappa < 0$. f_κ and g_κ are the solutions of the usual radial equations [23]. The mean field in the Dirac equation is determined through a Hartree procedure from a relativistic Lagrangian with scalar and vector S-V terms [24]. We use the parameters of Ref. [25], and the TIMORA code [26].

The wave function for the outgoing proton Ψ_F is a scattering solution of the Dirac equation (2.1), which includes S-V global optical potentials, as discussed in Sec. II. This wave function is obtained as a partial wave expansion in configuration space,

$$\Psi_F(\mathbf{r}) = 4\pi \sqrt{\frac{E_F + M}{2E_F}} \sum_{\kappa,\mu,m} e^{-i\delta_\kappa^*} i^l \langle l \ m \ \tfrac{1}{2} \ \sigma_F | j \ \mu \rangle \times Y_{lm}^*(\hat{P}_F) \Psi_\kappa^\mu(\mathbf{r}) \ , \tag{3.5}$$

where $\Psi_\kappa^\mu(\mathbf{r})$ are four-spinors of the same form as that in Eq. (3.3), except that now the radial functions f_κ, g_κ are complex because of the complex potential. It should also be mentioned that since the wave function (3.5) corresponds to an outgoing proton, we use the complex conjugates of the radial functions and phase shifts (the latter with the minus sign).

For the nucleon current operator we take the free nucleon expression

$$\hat{J}_N^\mu = F_1 \gamma^\mu + i \frac{\bar{\kappa} F_2}{2M} \sigma^{\mu\nu} q_\nu \ , \tag{3.6}$$

where F_1 and F_2 are the nucleon form factors related in the usual way [22] to the electric and magnetic Sachs form factors of the dipole form. As discussed in Refs. [11,27], DWIA results depend on the choice of the nucleon current operator. Here we have chosen the operator that is closer to the one used in the nonrelativistic calculations in the DWEEPY code.

The numerical calculations involve (i) computation of the radial functions in configuration space; (ii) numerical integration; and (iii) summation of partial waves. The accuracy of the numerical procedure is tested by comparison to the exact result in the plane wave limit (PWIA). Typically our calculations involve 30–40 partial waves for the ejected proton and numerical integration over a range of 15–20 fm in steps of 0.1 fm. The parameters (number of partial waves, radii, and step size of integration) are adjusted so that differences with exact PWIA cross sections are less than 0.1%. Finally, it should also be mentioned that recoil effects, though small, are taken into account by replacing $\mathbf{q}$ in Eq. (3.2) by $\mathbf{q}(A-1)/A$, and $\mathbf{P}_F$ by $[\mathbf{P}_F(A-1) + \mathbf{P}_{A-1}]/A$.

B. Nonrelativistic formalism

In the nonrelativistic formalism, the numerical calculations have been done with the code DWEEPY [4] that uses as input nonrelativistic optical potentials and bispinor bound nucleon wave functions. As already indicated, the calculations have been done switching off the Coulomb distortion of the electron wave functions. The nucleon current operator used in this code was obtained [5,28] through a Foldy-Wouthuysen procedure up to order $(p/M)^4$, based on the current operator in Eq. (3.6) for free nucleons satisfying the relation

$$\Psi_{\text{down}} = \frac{\boldsymbol{\sigma} \cdot \mathbf{p}}{E + M} \Psi_{\text{up}} \ . \tag{3.7}$$

Thus, at variance with the relativistic formalism, the nucleon current in Eq. (3.2) is calculated using a nonrelativistic current operator and bispinors for the initial (bound) and final (scattering) proton wave functions. The outgoing proton wave functions are obtained as solutions of the Schrödinger equation with the DEB and standard optical potentials defined in Sec. II. The bound proton wave functions are generally obtained as solutions of the Schrödinger equation with real central and spin-orbit Woods-Saxon type potentials [11]. However, for the nonrelativistic results presented here we have used instead the upper component of the relativistic bound nucleon wave function, normalized to 1. This minimizes

differences in the cross sections coming from the use of different bound nucleon wave functions in the relativistic and nonrelativistic formalisms. Indeed, we have checked that in this case both formalisms give the same results in PWIA (i.e., in the limit of no final state interactions). Thus, with this choice, we ensure that the differences among the various results presented here are solely due to differences in the outgoing nucleon wave functions generated from the different optical potentials. Though in principle in the nonrelativistic case one would take the upper component of the relativistic bound state wave function after projection of the positive energy part, in practice for the solutions of the TIMORA code this makes practically no difference (we shall come back to this point later on).

C. Discussion of results

In Figs. 3 and 4 we show the reduced cross sections $\rho(p)$, for proton knockout from the shells $3s_{1/2}$ and $2d_{3/2}$ in ^{208}Pb, respectively, obtained in various approximations as functions of the missing momentum p. The result of the relativistic calculation (solid line) is compared in each figure with the results of nonrelativistic calculations obtained with the standard (long dashed line) and DEB (dashed line) optical potentials. The dotted line shows the result obtained using the solution of the Schrödinger equation with the DEB potential multiplied by the factor $K(r)$.

One can clearly see in Figs. 3 and 4 that, taking the relativistic result as a reference, the large discrepancy found in the nonrelativistic calculations with the standard potential decreases substantially when using the DEB potential. As expected, the nonrelativistic result gets closer to the relativistic one when using the optical potential that gives an equivalent fit to elastic nucleon scattering. We recall that the standard potential is a particular 15-parameter fit to 46 data on elastic proton

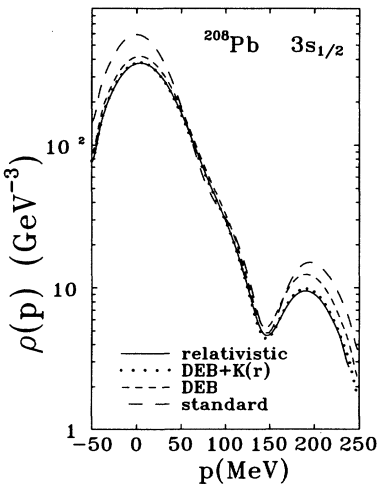

FIG. 3. Comparison of various $(e, e'p)$ reduced cross sections for the shell $3s_{1/2}$ of ^{208}Pb (see text).

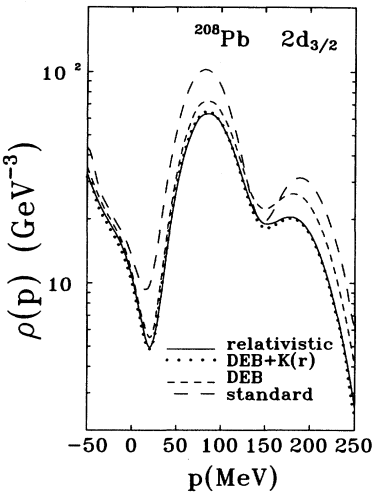

FIG. 4. Same as Fig. 3 for the shell $2d_{3/2}$.

scattering at 98 MeV from ^{208}Pb, while the relativistic potential (and hence the DEB potential) is a global fit over a wide range of proton energies and mass numbers involving more than 4000 data points. These two fits are not equivalent and hence it is not surprising that the two potentials—standard and DEB—differ (see Fig. 1) and produce different $(e, e'p)$ cross sections, the latter giving more absorption for the cases studied here.

This allows us to conclude that a large part of the discrepancy between relativistic and nonrelativistic results is reduced when using relativistic and nonrelativistic optical potentials that give equivalent fits to elastic proton-nucleus scattering. Yet, it is also clear from Figs. 3 and 4 that even with the DEB potential there are still sizable differences between the nonrelativistic result and the relativistic one. The latter is only recovered when the Darwin factor $K(r)$ is also taken into account. This means that the $(e, e'p)$ cross section is sensitive to the increased reduction in the nuclear interior of the relativistic outgoing nucleon density. This reduction is clearly seen when one plots the ratio between the relativistic $(\bar{\Psi}_F \gamma^0 \Psi_F)$ and the nonrelativistic $(\phi^\dagger \phi)$ density profiles. Said ratio is mainly given by the real part of $A(r)$ shown in Fig. 2. The effect of the Darwin factor is irrelevant to elastic proton-nucleus scattering but is important in $(e, e'p)$ processes that are sensitive to the nuclear interior.

One may wonder whether it is legitimate to use $K\phi$ when working within the nonrelativistic formalism and whether the above comparison is actually meaningful. It is easy to convince oneself that this is indeed the case when using the DWEEPY program as done here. The simplest way to show that is to consider the direct Pauli reduction [19,29] of the relativistic nucleon current. To carry out this reduction, four-component wave functions with only positive energy components are built,

$$\Psi_+(\mathbf{p}) = N_+(p) \begin{pmatrix} \Psi_{\rm up}(\mathbf{p}) \\ \dfrac{\boldsymbol{\sigma}\cdot\mathbf{p}}{E(p)+M}\Psi_{\rm up}(\mathbf{p}) \end{pmatrix}, \qquad (3.8)$$

out of the fully relativistic four-component wave func-

tions using the positive energy projection operator [22], and an effective nonrelativistic current operator $\hat{J}^{\mu}_{\rm nr}$ is defined such that

$$\bar{\Psi}^{F}_{+}\hat{J}^{\mu}_{N}\Psi^{B}_{+} = \Psi^{F\,\dagger}_{\rm up}\hat{J}^{\mu}_{\rm nr}\Psi^{B}_{\rm up} \tag{3.9}$$

with $\Psi^{B}_{\rm up}$ and $\Psi^{F}_{\rm up}$ the upper components of the relativistic initial and final wave functions. In practice, once the operator $\hat{J}^{\mu}_{\rm nr}$ is obtained the nonrelativistic current is calculated using initial and final wave functions that are solutions of ordinary Schrödinger equations.

It can be shown [29] analytically that to third order in (p/M) the operator in Eq. (3.9) $\hat{J}^{\mu}_{\rm nr}$ is identical to the nonrelativistic current operator obtained by the Foldy-Wouthuysen procedure and used in the code DWEEPY. We have also checked that up to fourth order the differences are negligible (less than 0.1% for the energies considered here). Equation (3.9) is then a useful bridge to understand the relationship between the relativistic results and the nonrelativistic ones with the DEB potential in Figs. 3 and 4, as well as its meaning.

To this end we first compare in Fig. 5 the fully relativistic results (solid line) for the $3s_{1/2}$ and $2d_{3/2}$ shells in ^{208}Pb with the results obtained with the relativistic code when using initial and final nucleon wave functions projected on the positive energy plane (dashed line). One can see that the differences between the results are small, being only noticeable at relatively high p. This shows that the coupling to the negative energy contributions of the Dirac solutions does not play an important role in the fully relativistic result and cannot be responsible for the observed discrepancies between the relativistic and nonrelativistic results in Figs. 3 and 4. It then follows, taking also into account Eq. (3.9) and the correspondence between $\hat{J}^{\mu}_{\rm nr}$ and the current operator used in DWEEPY, that in order to recover the relativistic result one has to use the upper components of the initial (bound) and final

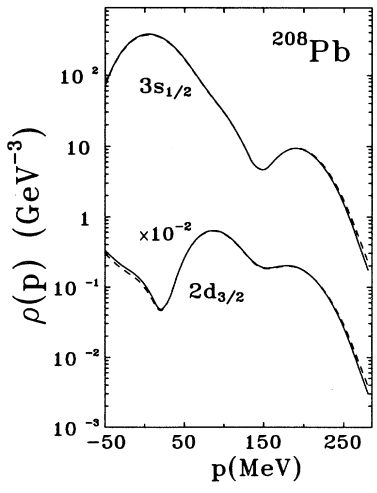

FIG. 5. Comparison of the fully relativistic results (solid lines) with results obtained after projection of initial and final nucleon wave functions on the positive energy plane (dashed lines).

(scattering) nucleon wave functions. This explains why in Figs. 3 and 4 the nonrelativistic calculations with the DEB potential reproduce the relativistic result once the factor $K(r)$ is taken into account.

Although not explicitly shown here, the situation is similar with regard to the bound nucleon wave function, i.e., if in the nonrelativistic calculation we use for the bound state the solution (ϕ_B) of the Schrödinger equation with the DEB potential corresponding to the relativistic S-V potential used in the TIMORA code, we have to take into account an extra factor $K_B(r)$. This reflects the fact that, as seen from Eqs. (2.9)–(3.9), the nonrelativistic current operator consistent with the nonrelativistic solutions of DEB potentials is related to that in the right-hand side of Eq. (3.9) by

$$\hat{J}^{\rm eff}_{\rm nr} = K^{*}(r)\hat{J}_{\rm nr}K_B(r)\ . \tag{3.10}$$

Since DWEEPY uses $\hat{J}_{\rm nr}$ rather than $\hat{J}^{\rm eff}_{\rm nr}$, we cannot recover the relativistic results when using $\phi(\mathbf{r})$ and/or $\phi_B(\mathbf{r})$ unless we insert the corresponding K factors. A similar remark was first pointed out in Ref. [30] in the context of photonuclear reactions, where the effect of the S-V potentials in the interaction Hamiltonian was studied up to second order in a $1/(E+M)$ expansion.

Clearly $\hat{J}^{\rm eff}_{\rm nr}$ depends on the relativistic potentials used in the calculations and for the purpose of comparing results obtained in the nonrelativistic framework, it is advantageous to stick to a single definition of the current operator, as that used by DWEEPY, adding the required modifications *a posteriori*. It should also be pointed out that in standard nonrelativistic analyses, the bound nucleon wave function fits observables (rms radii, binding energies, etc.) that depend on the nuclear interior. Thus, to the extent that this nonrelativistic wave function fits similar phenomenology as the fully relativistic one, the study of the effect of $K_B(r)$ is not as meaningful, for the purpose of this paper, as that of $K(r)$. This is why we focus here on $K(r)$.

It is interesting to compare the function $K(r)$ with the Perey factor (PF) as defined in Ref. [31]:

$$f(r) = \exp\left(\frac{1}{2}\beta^2\frac{M}{2\hbar^2}V_C\right)\ , \tag{3.11}$$

where β is a nonlocality range parameter and V_C is the central potential in Eq. (2.5). Analogous to $K(r)$, the PF produces also a reduction of the wave function in the nuclear interior. In fact, the PF calculated with the DEB potential has a similar shape to the function $K(r)$. It is worth pointing out that the need for the PF emerged from a completely different starting point. Namely, from the analysis of nonlocalities of the nonrelativistic optical potential, parametrized in terms of the nonlocality range parameter β.

In Fig. 6 we show the effect in the $(e,e'p)$ reduced cross section due to the inclusion of the PF $[f(r)]$. We show nonrelativistic results obtained with the DEB potential and compare them with the relativistic result. The results in this figure correspond to the $2d_{3/2}$ orbital in ^{208}Pb and to two values of the β parameter ($\beta = 0.85, 1.0$

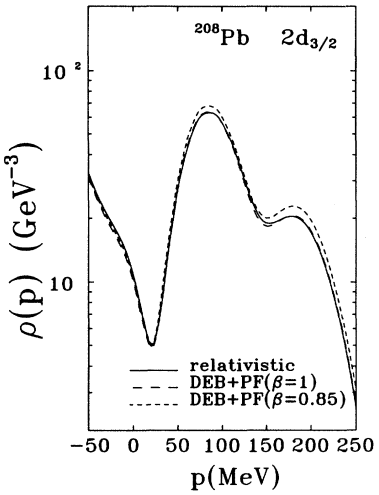

FIG. 6. Comparison of the relativistic $(e, e'p)$ reduced cross section to nonrelativistic ones obtained with the DEB potential and Perey factors for two values of the nonlocality parameter β (see text).

fm). As can be seen in the figure, the effect of the PF is similar to the effect of $K(r)$ shown and discussed in Figs. 3 and 4. Actually for $\beta = 1$ the result obtained with DEB+PF reproduces quite well the relativistic result. This is consistent with the fact that for this β value the depth (0.83) of the PF is comparable to the depth (0.79) of $K(r)$. With the most commonly used value of β ($\beta = 0.85$), the effect of the PF is not sufficient to reproduce the relativistic result.

We have checked that the effect of the PF for $\beta = 1$ with the DEB potential is similar to the effect of $K(r)$ also for the $3s_{1/2}$ orbital in ^{208}Pb and for the orbitals $2s_{1/2}$ and $1d_{3/2}$ in ^{40}Ca also considered in Ref. [11]. In Table II we summarize the results for all these orbitals. In this table we give, for each orbital and nucleus, the ratio between the nonrelativistic and the relativistic reduced cross sections at their maxima. Following the order of appearance in the table, the five nonrelativistic cases considered are (1) the standard optical potential (given in Ref. [2] for ^{208}Pb and in Ref. [3] for ^{40}Ca), (2) the DEB optical potential, (3) DEB including the Perey factor with $\beta = 0.85$, (4) DEB including the Perey factor with $\beta = 1$, and (5) DEB including $K(r)$. From this table it is clear that the trend observed in going from the standard optical potentials to the DEB+$K(r)$ case is similar for all the shells studied in Pb as well as in Ca. Compared to the relativistic calculation, the standard optical potentials produce too large $(e, e'p)$ cross sections with ratios between 1.2 and 1.6. These ratios are reduced to values between 1.1 and 1.3 when the DEB potential is used. The nonlocal corrections introduced by the Perey factor act in the right direction and the cross sections become closer to the relativistic results, particularly for $\beta = 1$, where the agreement with the relativistic result is comparable to that obtained with $K(r)$. With the inclusion of the function $K(r)$ the relativistic results are recovered within a reasonable 1% to 5% deviation.

At this point one may wonder if the similarity between the effect of $K(r)$ and PF for $\beta = 1$ fm could be regarded as more than a mere coincidence. Actually, also the function $K(r)$ is related to nonlocalities. Indeed, as explained in Appendix A, the function $K(r)$ appears when converting the Schrödinger-like equation with a nonlocal potential for Ψ_{up} into an ordinary Schrödinger equation with no first derivative terms. This agrees with the generally accepted notion that the relativistic approach may already include an important amount of nonlocal effects in the nonrelativistic formalism. Nonlocal terms in the nonrelativistic equation may be partly justified just as well as the spin-orbit terms in the nonrelativistic equation is justified by looking into the nonrelativistic limit of the Dirac equation. It is well known that the central potential derived from S-V potentials which are local and non-energy-dependent contains a linear dependence on the energy. The relativistic optical potentials themselves already contain some energy dependence, although relatively weak for the energies of interest here compared to the explicit energy dependence of the DEB potential shown in Eq. (2.5).

However, the analogy between the Perey and $K(r)$ factors has to be considered with caution until a rigorous study of the role of nonlocalities is made, starting from nonlocal analyses in both relativistic and nonrelativistic formalisms. This goes beyond the scope of this paper where we point out this numerical similarity as a "striking coincidence" that may encourage further work along these lines.

IV. SUMMARY AND FINAL REMARKS

In Ref. [11] we found that the relativistic optical potentials from Ref. [18] are able to explain simultaneously

TABLE II. Ratio between various nonrelativistic and the fully relativistic reduced cross sections for p values close to the maxima of the two outermost shells of ^{208}Pb and ^{40}Ca.

	^{208}Pb				^{40}Ca			
	$3s_{1/2}$		$2d_{3/2}$		$2s_{1/2}$		$1d_{3/2}$	
p (MeV)	0	190	100	180	0	150	−140	110
Standard	1.59	1.57	1.36	1.48	1.16	1.48	1.25	1.31
DEB	1.11	1.30	1.14	1.29	1.11	1.32	1.09	1.19
DEB nonlocal ($\beta = 0.85$)	1.06	1.14	1.07	1.11	1.06	1.14	0.99	1.13
DEB nonlocal ($\beta = 1.0$)	1.00	1.01	1.00	1.01	1.03	1.07	0.97	1.07
DEB $K(r)$	1.01	1.03	1.02	0.98	1.05	1.05	0.98	1.07

the elastic proton-nucleus scattering data and the $(e,e'p)$ cross sections, while the most commonly used nonrelativistic ones fail to do that with reasonable spectroscopic factors. As in previous work [11] the nonrelativistic calculations are done here with the code DWEEPY that uses as input local nonrelativistic optical potentials and bound nucleon wave functions. In this paper we investigate why the relativistic and the nonrelativistic optical potentials lead to different $(e,e'p)$ reduced cross sections, even though both are fitted to elastic proton-nucleus scattering data. To this end we have followed the already known procedure of building a nonrelativistic optical potential from the relativistic one that led to the same elastic scattering observables.

By this procedure we obtain a nonrelativistic optical potential (DEB), as well as a function $K(r)$ relating the upper component of the Dirac solution with the solution of the Schrödinger equation with the DEB potential. The function $K(r)$ is less than 1 in the nuclear interior and goes to 1 asymptotically. It is this latter fact that guarantees that the DEB potential fits equally as well as the relativistic one the elastic proton-nucleus scattering data at proton energies of our concern here.

We find that the DEB potential differs from the standard nonrelativistic potential and leads to lower $(e,e'p)$ cross sections. This reflects the fact that the two potentials correspond to nonequivalent fits of elastic proton-nucleus scattering. We find that the large discrepancy between the results of relativistic and nonrelativistic calculations is partly reduced when using the DEB optical potential, instead of the standard one, in the nonrelativistic formalism. This shows that better agreement between relativistic and nonrelativistic results is found when the potentials used give equivalent fits to elastic proton-nucleus scattering. Yet, even with the DEB potential the $(e,e'p)$ cross section turns out to be larger than the corresponding relativistic result. The latter is, however, recovered in the nonrelativistic calculation with DEB after inclusion of the function $K(r)$, showing the sensitivity of $(e,e'p)$ to the behavior of the wave functions in the nuclear interior.

The role of dynamically enhanced lower components is not relevant for the $(e,e'p)$ processes discussed here, as shown by the fact that the relativistic calculations produce nearly the same results independent of whether one uses the complete solutions of the Dirac equations for initial and final nucleons or one uses their positive energy projected counterparts. This is crucial to understand why the results obtained with the nonrelativistic formalism using the DEB potential and the Darwin factor $K(r)$ reproduce the results of the fully relativistic calculations within at most a 1–5% deviation.

The above-mentioned results reproduce the fully relativistic ones because they amount to a strict two-component reduction of the nuclear current in which negative energy contributions, which are small anyway in the $(e,e'p)$ processes, have been neglected. On the other hand if one forgets about the Darwin factor K and uses the function ϕ corresponding to the DEB potential when calculating the $(e,e'p)$ cross sections in the nonrelativistic framework, one finds a sizable deviation from the fully relativistic result. This is in contrast to the case of elastic proton scattering where the relativistic results are recovered with the DEB potential independent of whether the factor K is taken into account or not. Since the elastic proton-nucleus scattering data are only sensitive to the asymptotic behavior of the wave function, these experiments cannot provide information on the function $K(r)$ in the nuclear interior. Therefore, the behavior of this function, and its effects on observables sensitive to the nuclear interior, are predictions of the model.

We have compared the effect of the function $K(r)$ that has a relativistic origin with that produced by the Perey factor that simulates the effect of nonlocalities in the nonrelativistic optical potentials. We have shown that both functions produce nearly identical absorption for a nonlocality parameter $\beta = 1$ fm. Although at first sight it may look surprising that one arrives to similar effects from quite different starting points, one should keep in mind that also the function $K(r)$ can be related to nonlocalities. Indeed, when one replaces Eq. (2.9) into Eq. (2.3), one ends up with a Schrödinger equation with a nonlocal optical potential for the upper component of the Dirac solution (see Appendix A). Thus, both the $K(r)$ and the Perey factors can be interpreted as corresponding to contributions which give effective local representations of nonlocal effects.

Independently of the interpretation of $K(r)$, what we may undoubtedly conclude is the following. (i) If we compare the relativistic density for the outgoing nucleon $(\bar{\Psi}_F\gamma^0\Psi_F)$, obtained with the S-V potential of Ref. [18], to the naively defined nonrelativistic density $\phi^\dagger\phi$, obtained with the corresponding DEB potential, the former shows a depletion in the interior governed by $|K(r)|^2$. (ii) This depletion plays an important role in $(e,e'p)$ processes, and must be taken into account in nonrelativistic calculations performed with the DWEEPY code by introducing the Darwin factors, which appear in a proper nonrelativistic reduction of the nucleon current operator. Modifications of the interaction Hamiltonian for photonuclear reactions due to the S-V potentials have also been discussed in Ref. [30].

Recently, a paper by Jin and Onley [32] has appeared that also discusses comparisons between relativistic and nonrelativistic calculations for ^{40}Ca$(e,e'p)^{39}$K cross sections. The main conclusions of these authors seem to agree with ours. In their case the relationship between relativistic and nonrelativistic results and its comparison to the effect of the Perey factor are somewhat different due to the fact that they consider a different nonrelativistic scheme to the one considered here.

ACKNOWLEDGMENTS

One of us (J.M.U.) is carrying out the work as a part of a Community training project financed by the European Commission under Contract No. ERBCHBICT 920185 and thanks H.P. Blok for useful comments. This work was partially supported by DGICYT (Spain) under Contract No. 92/0021-C02-01.

APPENDIX A: DERIVATION OF THE SCHRÖDINGER EQUIVALENT EQUATION

Starting from the Dirac equation [Eq. (2.1)] we write

$$A_-\Psi_{\rm up} - \mathbf{p}\cdot\boldsymbol{\sigma}\Psi_{\rm down} = 0\,, \tag{A1}$$

$$A_+\Psi_{\rm down} - \mathbf{p}\cdot\boldsymbol{\sigma}\Psi_{\rm up} = 0\,, \tag{A2}$$

with

$$A_\pm = E - U_V - U_C \pm (M + U_S)\,. \tag{A3}$$

Applying $\mathbf{p}\cdot\boldsymbol{\sigma}$ to Eq. (A2) one gets

$$\boldsymbol{\nabla}^2\Psi_{\rm up} = -\mathbf{p}\cdot\boldsymbol{\sigma}A_+\Psi_{\rm down} = i\boldsymbol{\sigma}\cdot\hat{\mathbf{r}}\left(\frac{dA_+}{dr}\right)\Psi_{\rm down} - A_+\mathbf{p}\cdot\boldsymbol{\sigma}\Psi_{\rm down} \tag{A4}$$

using Eqs. (A1) and (A2) to eliminate $\Psi_{\rm down}$ from the second and first terms in the right-hand side of Eq. (A4), respectively, and using the identity

$$i\boldsymbol{\sigma}\cdot\hat{\mathbf{r}}\,\boldsymbol{\sigma}\cdot\mathbf{p} = \frac{d}{dr} - \frac{\boldsymbol{\sigma}\cdot\mathbf{l}}{r}\,, \tag{A5}$$

one gets

$$\left[\boldsymbol{\nabla}^2 + \frac{1}{A_+}\frac{dA_+}{dr}\frac{\boldsymbol{\sigma}\cdot\mathbf{l}}{r} + A_+A_- - \frac{1}{A_+}\frac{dA_+}{dr}\frac{d}{dr}\right]\Psi_{\rm up} = 0\,. \tag{A6}$$

This is an exact second order differential equation for $\Psi_{\rm up}$ that can be interpreted as a Schrödinger-like equation with a nonlocal potential. The Schrödinger equivalent equation and the DEB potential defined in Eqs. (2.3)–(2.8) is obtained after the elimination of the last term (Darwin term) in Eq. (A6). To this end one looks for a transformation, $\Psi_{\rm up}(\mathbf{r}) = K(r)\phi(\mathbf{r})$, under which Eq. (A6) transforms into an ordinary Schrödinger equation (i.e., with no first derivative terms) and such that $\Psi_{\rm up}(\mathbf{r})_{r\to\infty} \longrightarrow \phi(\mathbf{r})$. This determines $K(r)$ in Eq. (2.10).

[1] P.K.A. de Witt Huberts, J. Phys. G **16**, 507 (1990); L. Lapikás, Nucl. Phys. **A553**, 297c (1993).

[2] E.N.M. Quint, Ph.D. thesis, University of Amsterdam, 1988.

[3] G.J. Kramer, Phys. Lett. B **227**, 199 (1989); Ph.D. thesis, University of Amsterdam, 1990.

[4] C. Giusti and F. Pacati, Nucl. Phys. **A473**, 717 (1987); **A485**, 461 (1988); M. Traini, Phys. Lett. B **213**, 1 (1988).

[5] S. Boffi, C. Giusti, and F. Pacati, Nucl. Phys. **A336**, 416 (1980); C. Giusti and F. Pacati, *ibid.* **A336**, 427 (1980).

[6] A. Picklesimer, J.W. Van Orden, and S.J. Wallace, Phys. Rev. C **32**, 1312 (1985).

[7] A. Picklesimer and J.W. Van Orden, Phys. Rev. C **35**, 266 (1987).

[8] A. Picklesimer and J.W. Van Orden, Phys. Rev. C **40**, 290 (1989).

[9] J.P. McDermott, Phys. Rev. Lett. **65**, 1991 (1990).

[10] Y. Jin, D.S. Onley, and L.E. Wright, Phys. Rev. C **45**, 1311 (1992).

[11] J.M. Udías, P. Sarriguren, E. Moya de Guerra, E. Garrido, and J.A. Caballero, Phys. Rev. C **48**, 2731 (1993).

[12] V.R. Pandharipande, C.N. Papanicolas, and J. Wambach, Phys. Rev. Lett. **53**, 1133 (1984); Z.Y. Ma and J. Wambach, Phys. Lett. B **256**, 1 (1991); C. Mahaux and R. Sartor, Adv. Nucl. Phys. **20**, 1 (1991).

[13] G.J. Wagner, Prog. Part. Nucl. Phys. **24**, 17 (1990).

[14] H.S. Sherif, R.I. Sawafta, and E.D. Cooper, Nucl. Phys. **A449**, 709 (1986).

[15] S. Boffi, C. Giusti, F.D. Pacati, and F. Cannata, Nuovo Cimento **98**, 291 (1987).

[16] H.P. Blok, L.R. Kouw, J.W.A. den Herder, L. Lapikás, and P.K.A. de Witt Huberts, Phys. Lett. B **198**, 4 (1987).

[17] L. Ray, G.W. Hoffmann, and W.R. Coker, Phys. Rep. **212**, 223 (1992), and references therein.

[18] S. Hama, B.C. Clark, E.D. Cooper, H.S. Sherif, and R.L. Mercer, Phys. Rev. C **41**, 2737 (1990).

[19] E.D. Cooper, S. Hama, B.C. Clark, and R.L. Mercer, Phys. Rev. C **47**, 297 (1993).

[20] J.M. Udías, Ph.D. thesis, Universidad Autónoma de Madrid, 1993.

[21] S. Frullani and J. Mougey, Adv. Nucl. Phys. **14**, 1 (1984).

[22] J.D. Björken and S.D. Drell, *Relativistic Quantum Mechanics* (McGraw Hill, New York, 1964).

[23] M.E. Rose, *Relativistic Electron Theory* (Wiley, New York, 1961).

[24] B.D. Serot and J.D. Walecka, Adv. Nucl. Phys. **16**, 1 (1986).

[25] C.J. Horowitz and B.D. Serot, Nucl. Phys. **A368**, 503 (1981); Phys. Lett. **86B**, 146 (1979).

[26] C.J. Horowitz, D.P. Murdock, and B.D. Serot, in *Computational Nuclear Physics*, edited by K. Langanke, J.A. Maruhn, and S.E. Koonin (Springer-Verlag, Berlin, 1991).

[27] C.R. Chinn and A. Picklesimer, Nuovo Cimento **105A**, 1149 (1992).

[28] K.V. McVoy and L. van Hove, Phys. Rev. **125**, 1034 (1962).

[29] H.W. Fearing, G.I. Poulis, and S. Scherer, Nucl. Phys. **A570**, 657 (1994).

[30] M. Hedayati-Poor and H.S. Sherif, Phys. Lett. B **326**, 9 (1994).

[31] F. Perey and B. Buck, Nucl. Phys. **32**, 353 (1962); H. Fiedeldey, *ibid.* **77**, 149 (1966); M.M. Giannini and G. Ricco, Ann. Phys. (N.Y.) **102**, 458 (1976).

[32] Y. Jin and D.S. Onley, Phys. Rev. C **50**, 377 (1994).